Proc. Natl. Acad. Sci. USA
Vol. 95, pp. 10820–10825, September 1998
Medical Sciences

Endothelial cell death, angiogenesis, and microvascular function after castration in an androgen-dependent tumor: Role of vascular endothelial growth factor

(vascular regression/permeability/vascular density)

RAKESH K. JAIN*†, NINA SAFABAKHSH*‡, AXEL SCKELL*§, YI CHEN*, PING JIANG*, LAURA BENJAMIN¶, FAN YUAN*‖, AND ELI KESHET¶

*Edwin L. Steele Laboratory, Department of Radiation Oncology, Harvard Medical School and Massachusetts General Hospital, Boston, MA 02114; and ¶Department of Molecular Biology, The Hebrew University, Hadassah Medical School, Jerusalem, 91120, Israel

Edited by Webster K. Cavenee, University of California, La Jolla, CA, and approved June 26, 1998 (received for review March 27, 1998)

ABSTRACT **The sequence of events that leads to tumor vessel regression and the functional characteristics of these vessels during hormone–ablation therapy are not known. This is because of the lack of an appropriate animal model and monitoring technology. By using *in vivo* microscopy and *in situ* molecular analysis of the androgen-dependent Shionogi carcinoma grown in severe combined immunodeficient mice, we show that castration of these mice leads to tumor regression and a concomitant decrease in vascular endothelial growth factor (VEGF) expression. Androgen withdrawal is known to induce apoptosis in Shionogi tumor cells. Surprisingly, tumor endothelial cells begin to undergo apoptosis before neoplastic cells, and rarefaction of tumor vessels precedes the decrease in tumor size. The regressing vessels begin to exhibit normal phenotype, i.e., lower diameter, tortuosity, vascular permeability, and leukocyte adhesion. Two weeks after castration, a second wave of angiogenesis and tumor growth begins with a concomitant increase in VEGF expression. Because human tumors often relapse following hormone–ablation therapy, our data suggest that these patients may benefit from combined anti-VEGF therapy.**

Nearly one-third of human tumors are hormone sensitive. Hormone–ablation therapy leads to regression of the hormone-dependent tumors. In addition, hormone withdrawal inhibits vascular endothelial growth factor (VEGF) expression as well as angiogenesis in prostate cancer in both patients and animals (1, 2), and induces apoptosis in these cells during the regression (3–5). Shionogi murine tumor is a male mammary carcinoma and androgen-dependent. Similar to human hormone-sensitive tumors, the depletion of androgen by castration leads to regression of Shionogi tumors (3). Similar to human and murine hormone-dependent tumors, Shionogi tumor relapses after the regression following hormone ablation.

A more effective treatment would require an understanding of molecular and physiological processes during tumor growth, regression, and relapse. The mechanisms of rapid vascular regression following hormone withdrawal, the function of regressing vessels, and the molecular determinants responsible for the second wave of angiogenesis and tumor growth are, however, not known. In an effort to dissect these processes and to assess their clinical implications, we investigated angiogenesis, microvascular function, apoptosis, and VEGF expression during the initial growth, regression, and relapse of the Shionogi tumor. VEGF is expressed at a high level during the initial tumor growth and decreases to an almost undetectable level 1 week after castration. Strikingly, tumor endothelial cells begin to undergo apoptosis before neoplastic cells, the regressing vessels in the tumor begin to exhibit normal phenotype, and the dominant angiogenic factor in the relapsed tumor is VEGF.

MATERIALS AND METHODS

Tumor Model. Shionogi tumors were grown in male severe combined immunodeficient mice (6–8 weeks old, 25–35 g) bred and housed in our defined-flora animal colony. A dorsal skin-fold chamber was implanted under anesthesia [75 mg ketamine hydrochloride (Parke-Davis) and 25 mg xylazine (Fermenta, Kansas City, MO) per kg body weight, s.c.] as described (6). Animals were allowed to recover from the surgery for 2–3 days after implantation of the chamber. A 1-mm diameter fragment of the Shionogi tumor was implanted at the center of the dorsal chamber. This model allows quantitation of angiogenesis and microvascular function in the tumor for 30–40 days. Castration of animals was performed on day 15 or day 16 after tumor implantation through an abdominal incision under anesthesia (3).

Five to 12 animals were used for each parameter (tumor size, microvascular hemodynamics, vascular permeability, and leukocyte adhesion to tumor vessels). These parameters were measured during different phases of growth in castrated and sham-operated animals (Table 1). Vessel diameter and erythrocyte velocity were measured in about 100 vessels at each time point.

Measurement of Tumor Growth, Angiogenesis, and Hemodynamics. Animals with a dorsal skin-fold chamber were anesthetized (75 mg ketamine hydrochloride and 25 mg xylazine per kg body weight, s.c.) and placed in a polycarbonate tube. The chamber preparation was mounted on the microscope stage (Axioplan; Zeiss) and was observed by using a ×20 objective (LD acroplan; Zeiss). For measurement of vessel diameters and erythrocyte velocity, fluorescein isothiocyanate (FITC)-labeled dextran solution (5% in 0.9% NaCl) was injected i.v. as a bolus (4 ml/kg). Epi-illumination was achieved with a 100 W mercury lamp with fluorescence filters for FITC (excitation: 525–555 nm, emission: 580–635 nm). Images of

The publication costs of this article were defrayed in part by page charge payment. This article must therefore be hereby marked "*advertisement*" in accordance with 18 U.S.C. §1734 solely to indicate this fact.

This paper was submitted directly (Track II) to the *Proceedings* office.
Abbreviations: VEGF, vascular endothelial growth factor; TUNEL, terminal deoxynucleotidyltransferase-mediated UTP end labeling.
†To whom reprint requests should be addressed. e-mail: jain@steele.mgh.harvard.edu.
‡Present address: Kresge Building, Box 512, Temple University School of Medicine, 3420 North Broad Street, Philadelphia, PA 19140.
§Present address: Department of Orthopedic Surgery, University of Berne, Inselspital, CH-3010 Berne, Switzerland.
‖Present address: Department of Biomedical Engineering, Duke University, Box 90281, Durham, NC 27708-0281.

Table 1. Angiogenesis, microvascular hemodynamics, vascular permeability, and leukocyte rolling and adhesion in growing and regressing Shionogi tumors

Day		Tumor size,* mm^2	Vascular density,‡ cm/cm^2	Vessel diameter, μm	Erythrocyte velocity, mm/sec	Permeability,‡ $\times 10^{-7}$ cm/sec	Rolling count,§ %	Sticker,§ cells per mm^2	White blood cell flux,§ cells per mm^2/sec
7									
	Sham	3.5 (1.0)	53 (11)	22.7 (1.9)	0.12 (0.04)	2.5 (1.3)	31.6 (9.1)	237 (123)	1.52 (0.87)
		3.8 (1.7–5.0)	54 (25–78)	19.6 (4.3–50.9)	0.11 (0.03–0.19)	2.6 (0.8–4.2)	31.8 (18.4–43.1)	195 (77–418)	1.42 (0.75–3.30)
	Castr	NM	37 (15)	22.2 (5.0)	0.15 (0.07)	2.0 (1.2)	32.7 (9.0)	195 (222)	3.78 (3.76)
			37† (13–68)	21.8 (4.8–66.1)	0.15 (0.03–0.36)	2.0 (0.6–3.4)	31.3 (19.4–47.0)	85 (0–516)	2.31 (0.87–11.03)
14									
	Sham	5.8 (1.0)	101 (39)	36.7 (3.0)	0.16 (0.05)	2.3 (1.5)	34.0 (16.4)	306 (268)	1.88 (0.66)
		5.8 (4.3–7.8)	88 (53–194)	29.7 (8.5–94.4)	0.16 (0.06–0.27)	1.9 (1.0–5.6)	35.3 (9.9–55.8)	210 (0–788)	1.73 (1.09–2.88)
	Castr	NM	60 (13)	38.3 (6.7)	0.15 (0.06)	1.9 (0.7)	26.4 (10.1)	317 (229)	2.08 (1.25)
			59† (38–90)	40.6 (8.6–74.2)	0.15 (0.03–0.32)	2.3 (1.1–2.5)	28.9 (9.0–37.0)	292 (37–586)	1.81 (0.46–3.68)
18									
	Sham	7.1 (0.8)	87 (43)	45.7 (12.7)	0.17 (0.06)	NM	40.6 (4.5)	305 (116)	2.11 (0.98)
		7.1 (5.5–8.5)	67 (49–182)	34.2 (7.8–143.3)	0.15 (0.09–0.34)		41.9 (33.7–46.2)	301 (198–548)	2.05 (0.85–3.74)
	Castr	6.3 (0.8)	60 (23)	26.7 (2.8)	0.14 (0.06)	0.6 (0.1)	20.1† (6.1)	213 (121)	2.71 (1.37)
		6.5† (4.7–7.1)	60 (21–124)	23.9† (2.4–67.0)	0.15 (0–0.25)	0.6 (0.5–0.7)	21.3 (10.7–25.8)	209 (79–349)	2.70 (1.04–4.99)
23									
	Sham	10.1 (1.3)	112 (40)	48.4 (14.7)	0.15 (0.08)	2.5 (1.8)	42.0 (5.9)	365 (204)	2.11 (1.11)
		10.1 (8.3–12.9)	104 (48–208)	36.7 (8.6–94.7)	0.15 (0–0.34)	2.0 (0.82–5.6)	41.4 (34.0–48.7)	404 (0–606)	1.87 (0.98–3.88)
	Castr	5.9 (0.8)	53 (36)	15.0 (5.6)	0.14 (0.07)	1.2 (1.5)	23.3† (6.2)	258 (158)	3.77 (1.31)
		6.0† (4.5–7.5)	45† (12–188)	15.3† (2.0–76.6)	0.14 (0–0.32)	0.7† (0.5–4.8)	23.0 (16.2–31.0)	280 (29–435)	3.92 (1.81–5.37)
28									
	Sham	13.2 (1.0)	131 (50)	52.8 (13.4)	0.13 (0.05)	3.4 (1.7)	37.9 (8.2)	575 (206)	1.94 (0.97)
		13.4 (11.6–14.4)	121 (50–226)	45.2 (15.0–91.0)	0.13 (0–0.28)	3.1 (1.4–5.9)	39.9 (25.0–51.3)	627 (310–788)	2.06 (0.23–3.02)
	Castr	4.2 (0.6)	16 (19)	9.4 (7.4)	0.08 (0.09)	0.7 (0.5)	29.1 (10.7)	305† (213)	2.67 (0.46)
		4.4† (3.0–5.0)	10† (0–103)	12.8† (1.0–50.2)	0.11 (0–0.26)	0.6† (0.2–1.2)	26.1 (17.1–46.3)	284 (35–587)	2.71 (1.96–3.25)

Animals were divided into two groups: sham operated (Sham) or castrated (Castr) on day 15 or day 16. Measured data are expressed as mean (SD) as well as median (range). NM, no measurement.

*(*i*) Tumor surface area shown on days 7 and 28 was actually measured on days 8 and 29, respectively.
(*ii*) Tumor growth before day 8 was also quantified. Mean (SD) and median (range) (mm^2) were as follows: 1.83 (0.37) and 1.8 (1.2–2.8) on day 4; 2.6 (0.9) and 2.5 (1.5–4.2) on day 6.

†Indicating $P < 0.05$ in statistical analyses. One-way repeated measures analysis of variance and Student–Newman–Keuls tests were used for multiple comparisons in leukocyte–endothelial interaction studies. Mann–Whitney *U* test was used for comparing the differences between Sham and Castr groups.

‡The vascular density and permeability shown on day 18 were actually measured on day 17.

§Although average vessel diameter decreased after castration, for leukocyte–endothelial interaction analysis, only 100 μm vessel segments with diameters between 13 and 30 μm were chosen. Furthermore, all vessels chosen were straight and with confluent blood flow, indicating venule-like vessels. Erythrocyte-velocity measured in these vessel segments did not differ between groups (data not shown) and thus shear rate on the endothelial cell membrane did not differ between Sham and Castr groups. Mean (SD) and median (range) values on day 28 were as follows: (*i*) 0.12 (0.01) and 0.11 (0.10–0.13) (Sham); 0.13 (0.03) and 0.13 (0.10–0.16) (Castr) for erythrocyte velocity (mm/sec). (*ii*) 21.6 (5.4) and 20.3 (15.3–30.2) (Sham); 18.2 (2.35) and 18.3 (15.2–20.5) (Castr) for vessel diameter (μm). (*iii*) 47.9 (13.2) and 48.4 (30–66) (Sham); 58.4 (6.2) and 61.0 (50.5–64.3) (Castr) for shear rate (1/sec).

microvessels in five areas of the tumor were acquired by using a CCD camera (AVC D7; Sony, Tokyo), displayed on a video monitor and recorded on video tapes using a video recorder (SVO-9500MD; Sony) for off-line analysis.

Functional capillary density (an index of angiogenesis), defined as the total length of vessel with plasma flow per unit area of observation, and tumor surface area were measured using National Institutes of Health IMAGE software after digitization of images from video tape on a Macintosh computer (6). Erythrocyte velocities were measured by using a four-slit method (Microflow System, model 208C, video photometer version; IPM, San Diego) connected to a personal computer (IBM PS/2, 40 SX, Computer Land, Boston). The diameter of vessels was measured by using an image shearing device (digital video image shearing monitor, model 908; IPM) (6).

Microvascular Permeability Measurements. Tetramethylrhodamine-labeled bovine serum albumin (Molecular Probes; excitation peak at 541 nm, emission peak at 572 nm) was dissolved in PBS (6.5 mg/ml) and injected i.v. as a bolus (40 mg/kg). Fluorescence intensity in the selected area with a ×20 objective was quantified every 2 min over a period of 20 min by a photomultiplier (9203B; Thorn EMI Electron Tubes, Rockaway, NJ). These data were analyzed to estimate microvascular permeability to albumin as described earlier (7).

Leukocyte–Endothelial Interaction Measurements. Mice were injected with a bolus (20 μl) of 0.1% rhodamine 6-G in 0.9% saline through the tail vein to visualize leukocytes via an intensified CCD camera and recorded on a S-VHS tape. Only 100 μm segments of straight vessels with diameters between 13 and 30 μm were chosen for leukocyte studies. The numbers of rolling (Nr) and adhering (Na) leukocytes were counted for 30 sec along a 100 μm segment of a vessel. The total number of nonadhering leukocytes for 30 sec was also measured (Nt) to calculate the white blood cell flux (cells per unit time per unit vessel cross-sectional area) = $10^6 \times \mathrm{Nt}/(30\ \mathrm{sec} \times \pi \times D^2/4)$. The equations for calculating the ratio of rolling cells to Nt (rolling count), the density of adhering leukocytes (adhesion density), and the shear rate for each vessel are as follows: rolling count (%) = $100 \times \mathrm{Nr}/\mathrm{Nt}$, adhesion density (cells per mm^2) = $10^6 \times \mathrm{Na}/(\pi \times \mathrm{D} \times 100\ \mu\mathrm{m})$, shear rate = $8 \times \mathrm{Vmean}/D$ (8).

Histochemistry and *in Situ* Analyses. The tumor and the underlying subcutaneous tissue were excised from the chamber

and fixed in 4% formaldelyde. Formalin-fixed tumors were embedded in paraffin and cut into 4 μm sections for histochemistry and *in situ* analyses. Blood vessels were visualized by incubation with the *Bandeira simplicifolia* isolectin B4 (biotin-conjugated, Sigma) overnight, followed by incubation with extra-avidin-peroxidase (BioMakor, Rehovot, Israel; 1:20 dilution) and staining with 3-amino-9-ethylcabazole. *In situ* terminal deoxynucleotidyltransferase-mediated UTP end labeling (TUNEL) assays and *in situ* hybridization of tumor sections were performed as described (9, 10).

Northern Blot Analysis. VEGF mRNA was measured by using the procedure described in ref. 7. Briefly, total RNA was isolated from Shionogi tumor grown in severe combined immunodeficient mice by Trizol reagents (Life Technologies, Grand Island, NY) following the manufacturer's instructions. Fifteen micrograms of total RNA from each sample was electrophoresed through 1% agarose gel containing 40 mM 4-morpholinepropanesulfonic acid, 2 mM EDTA (pH 7.5), 5 mM iodoacetamide, and 2.2 M formaldehyde. Following electrophoresis, the fractionated RNAs were transferred to nylon membranes and hybridized with a DNA probe labeled with α-^{32}P (deoxyCTP). The β-actin expression was used as internal control.

RESULTS AND DISCUSSION

Dynamics of Tumor and Vessel Regression. The growth of Shionogi tumor in the dorsal skin-fold chambers is shown in Fig. 1. The transparent window model permits noninvasive monitoring of tumor growth, angiogenesis, and microvascular function for about 1 month (6). Animals were sham-operated or castrated on day 15 or day 16 after tumor implantation. In sham-operated animals, tumors expanded from 3.5 mm^2 surface area to 13 mm^2 in 3 weeks, with a concomitant increase in functional capillary density (angiogenesis) from $\approx$53 to $\approx$130 (cm/cm^2) (Table 1). In castrated animals, blood vessels in the tumor periphery began to regress within 24 hr of castration, and the tumors began to regress within 1–2 days. Note that in castrated animals, the capillary density was significantly lower before castration than the corresponding sham controls (Table 1). This is presumably because of heterogeneity in angiogenesis in these tumors. Nevertheless, the relative decrease in capillary density was significant ($P < 0.05$). More specifically, the tumor size decreased to about two-thirds and the capillary density decreased to about one-fifth, 2 weeks after castration compared with the same group of tumors at the time of castration (Table 1).

Mechanism of Vessel Regression. To identify the mechanism of rapid vascular regression following castration, we examined apoptosis in tumors by using *in situ* 3′ nick-end labeling (TUNEL). Shionogi carcinoma cells bear androgen receptors and are known to undergo apoptosis following hormone depletion (3–5). Surprisingly, we found TUNEL-positive endothelial cells on day 1 after castration, whereas the neoplastic cells were still TUNEL-negative (Fig. 2). We confirmed that the TUNEL-positive cells were indeed endothelial cells by labeling an adjacent thin section with a lectin stain (Fig. 2). From day 2 on, both the endothelial and neoplastic cells became TUNEL-positive. On day 6 we observed massive apoptosis throughout the tumor. In contrast, during physiological regression of blood vessels in regressing corpus luteum very few endothelial cells are TUNEL-positive compared with the luteal cells ($\approx$1:100) (11, 12).

We then investigated the mechanism of endothelial apoptosis. By using a tetracycline-regulated VEGF expression system in xenografted C-6 glioma cells, Benjamin and Keshet (13) have recently shown that turning off VEGF production leads to detachment of endothelial cells from tumor vessels and their subsequent death by apoptosis. VEGF is known to be a survival factor for endothelial cells (8). We therefore hypothesized that hormone ablation leads to a decrease in the production of VEGF by Shionogi cells. VEGF transcription began to decrease following castration, became about one-half by 24 hr, and was almost undetectable around day 7 after castration (Fig. 3 *A* and *B*). *In situ* hybridization analysis showed a uniform level of VEGF throughout the tumor before castration (Fig. 3*C*), whereas VEGF expression was down except for punctate VEGF expression at 24 hr after castration (Fig. 3*D*). The punctate pattern attests to differences in the level of expression between different cells, presumably because of microenvironmental differences. Onset of apoptosis at reduced ($\approx$50%) levels of VEGF at 24 hr suggests that a critical VEGF threshold is required for its endothelial survival function. This is supported by the heterozygous lethality of the VEGF knockout mice (14, 15). Taken together, these data show that androgen withdrawal downregulates VEGF production by androgen-dependent Shionogi cells. Tumor endothelial cells are presumably more dependent on VEGF for their

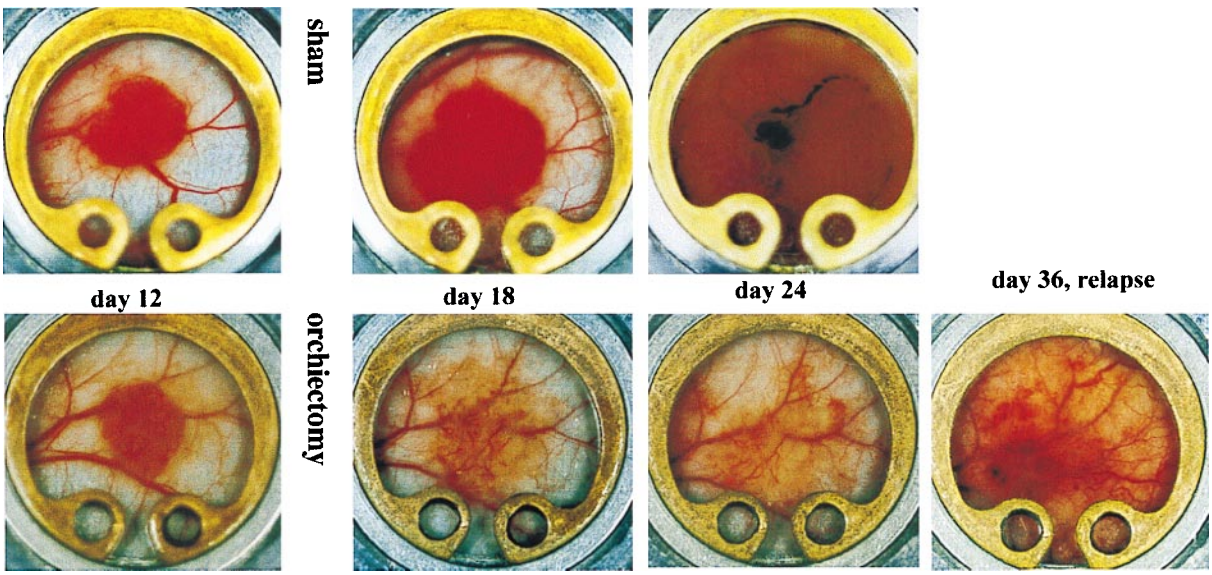

FIG. 1. Tumor growth and angiogenesis in Shionogi male mammary carcinomas. (*Upper*) Before castration (day 12) and in sham-operated animals (days 18 and 24). (*Lower*) Before castration (day 12), during regression in castrated animals (days 18 and 24), and during relapse (day 36). Note decreased angiogenesis in regressing tumor and second wave of angiogenesis in relapsed tumors.

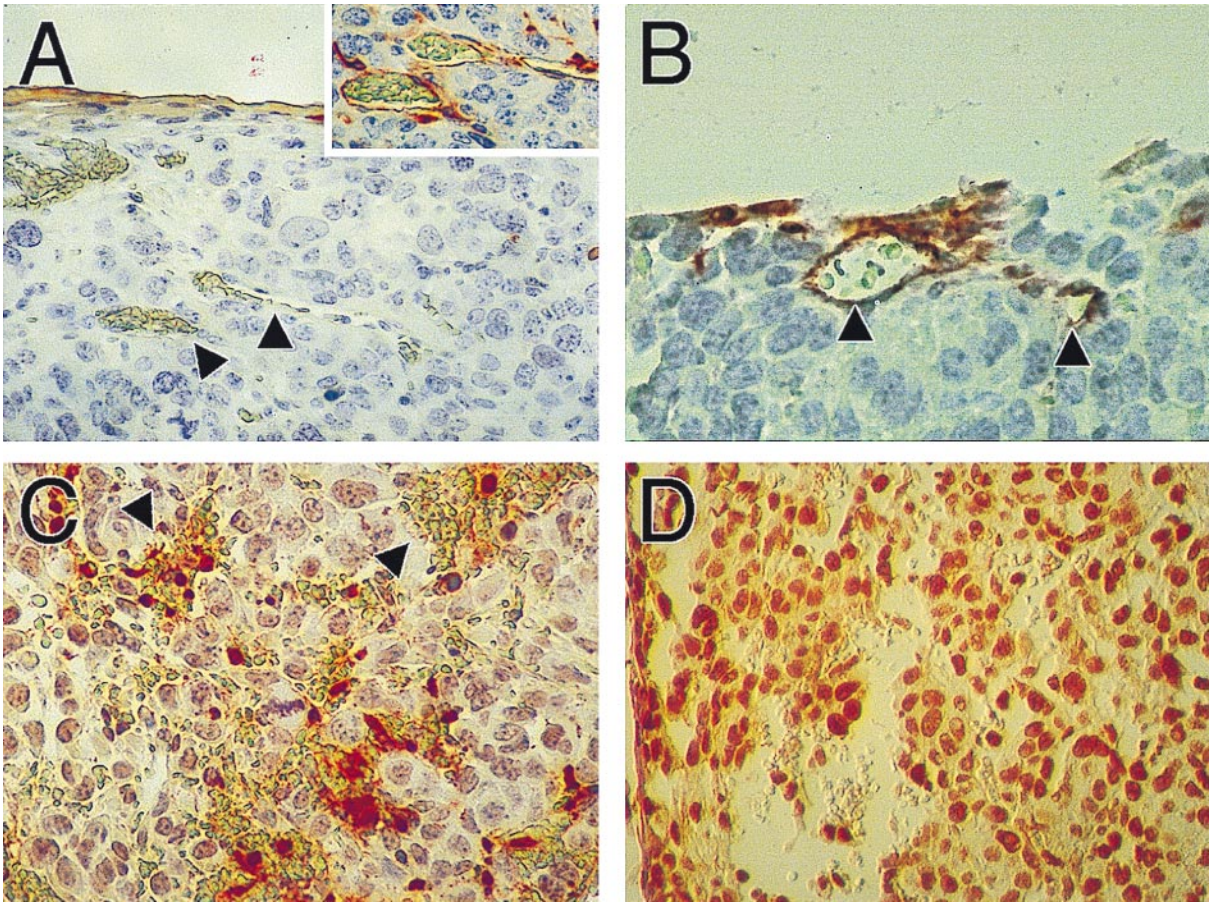

FIG. 2. TUNEL analysis of tumors shows death of endothelial cells following castration, but preceding death of tumor cells. (*A*) Control tumors show absence of apoptosis in blood vessels. *Inset* confirms the integrity of blood vessels shown by arrows using lectin staining to visualize the endothelial cell lining on an adjacent slide. (*B*) TUNEL-positive blood vessels are seen 24 hr after castration, whereas the majority of tumor cells remain TUNEL-negative. Arrows show blood vessels identified on the basis of lumen filled with erythrocytes. (*C*) Forty-eight hours after castration, more TUNEL-positive cells are found in regions of hemorrhaging blood vessels. Arrows show pools of erythrocytes that are not surrounded by intact endothelium. Still, most tumor cells are TUNEL-negative. (*D*) By 6 days after castration, intact blood vessels are not seen and tumor cells are TUNEL-positive.

survival than are the Shionogi cells on androgen. Therefore, endothelial cells begin to apoptose before cancer cells following castration.

Functional Characteristics of Regressing Vessels. A hallmark of regressing tumor vessels following VEGF neutralization with a blocking antibody is a decrease in their diameter (10). We found a striking resemblance between regressing Shionogi vessels and those regressing following anti-VEGF antibody treatment. The median diameter of Shionogi vessels decreased by ≈70% from 40.4 μm (before castration) to 12.8 μm, 2 weeks after castration (Table 1). In contrast, in control animals the vessel diameter increased to 45.2 μm on day 29 after tumor implantation. In addition, the regressing vessels became less tortuous, as demonstrated by a decrease in their minimum path length (16). Interestingly, vessel regression during luteolysis in the ovary involves contraction and occlusion of arterioles and small arteries with pronounced proliferation of smooth muscle cells (12). We did not see such occlusion in regressing Shionogi vessels, presumably because of a lack of functioning smooth muscle cells or pericytes in these tumor vessels. Indeed, the erythrocyte velocity in tumor vessels during growth and regression remained fairly constant (≈0.11–0.15 mm/sec). Thus, death of Shionogi cells was caused primarily by hormone withdrawal, and not reduced perfusion.

To gain further insight into the role of VEGF in regressing vessels, we measured vascular permeability to albumin in the tumor vessels. VEGF is a potent permeability enhancing factor (17). Based on our work on anti-VEGF antibody-induced regression (10), we anticipated a decrease in vascular permeability during regression. Vascular permeability increased in all animals during initial growth for up to 2 weeks. However, vascular permeability decreased within 2 days of castration and continued to decline for the next 2 weeks. In contrast, vascular permeability did not go down in control animals (Table 1). This finding is consistent with a decrease in pore size in vessels of Shionogi tumor after castration (18) and has significant clinical implications. For example, decrease in vascular permeability during regression would make it difficult to deliver therapeutic agents to neoplastic cells in the extravascular space during hormone–ablation therapy.

We then examined leukocyte adhesion in regressing vessels. We have recently shown that VEGF upregulates the expression of adhesion molecules, ICAM-1 and VCAM-1, on human umbilical vein endothelial cells *in vitro* and increases rolling and adhesion of leukocytes *in vivo* (7, 19). The effect of VEGF neutralization or downregulation on leukocyte adhesion, however, is not known. We hypothesized that the lower expression of VEGF in regressing tumors should lower leukocyte adhesion in vessels. We found a decrease, compared with sham-operated animals, in leukocyte rolling in Shionogi vessels 2 and 7 days after castration (Table 1). It is tempting to speculate that this decreased recognition of regressing tumor vessels by the host immune cells may contribute to their regrowth and thus tumor relapse.

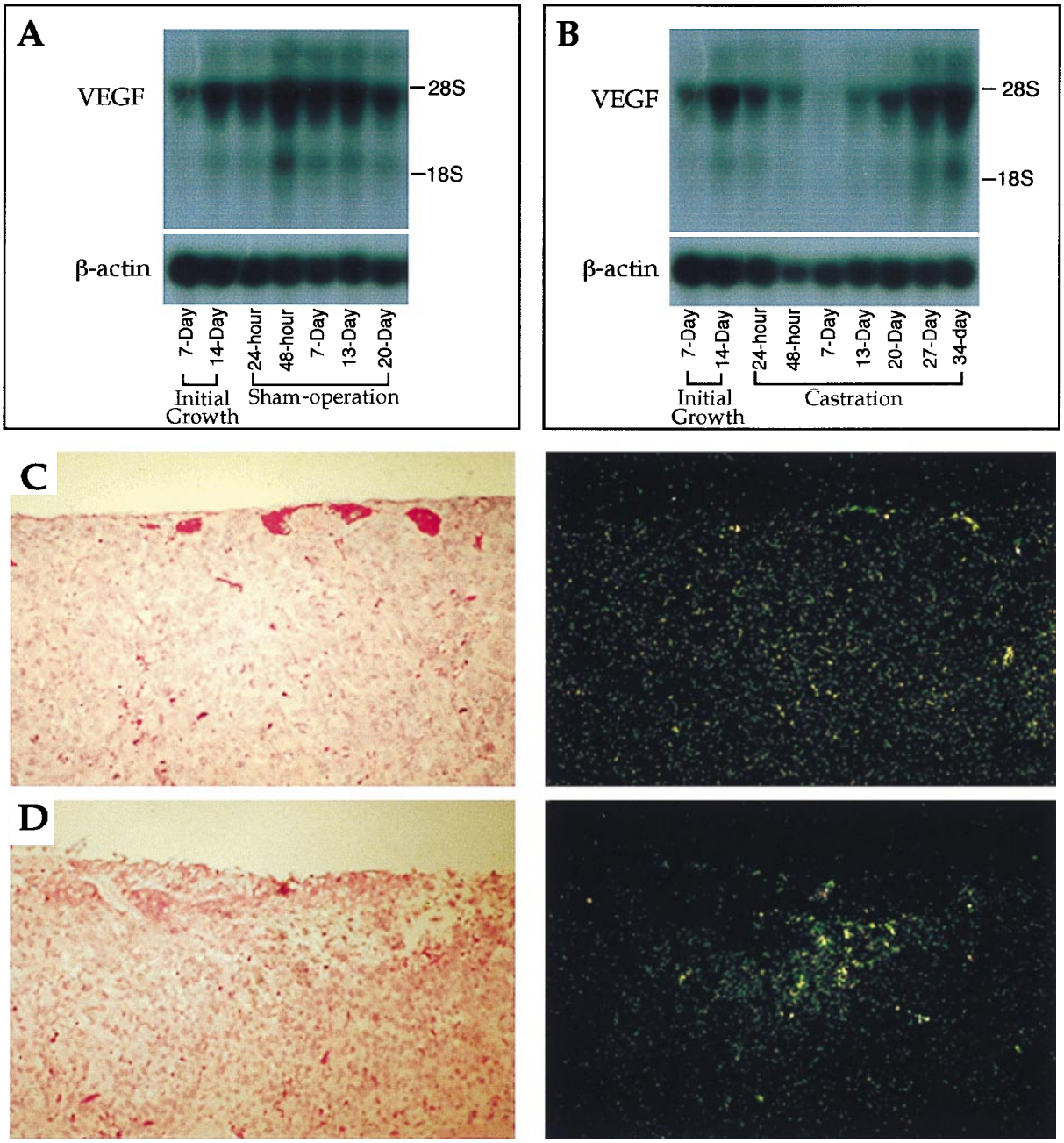

FIG. 3. VEGF expression in tumors by Northern blot analysis (*A* and *B*) and *in situ* hybridization (*C* and *D*). (*A* and *B*) During the initial growth, total RNA was isolated from the tumors at 7 and 14 days after implantation of tumors. The sham operation and castration were performed on day 15 of initial growth. Total RNA was isolated from tumors at the time points of 24 and 48 hr, and 7, 13, 20, 27, and 34 days after surgery. The levels of VEGF mRNA steadily increased in control (sham-operated animals; *A*). In contrast, the VEGF messages dramatically decreased and became almost undetectable on day 7 in tumors in castrated animals (*B*). However, the transcription of VEGF began to be upregulated on day 13 after castration and steadily increased to the level that was indistinguishable from that of the control (*B*). (*C*) Control tumor brightfield (*Left*) and darkfield (*Right*) show homogeneous levels of VEGF expression. (*D*) Twenty-four hours after castration brightfield (*Left*) and darkfield (*Right*) show punctate expression characteristic of stress-induced VEGF expression, but VEGF expression level is lower elsewhere.

Second Wave of Tumor Angiogenesis and Growth. Human tumors invariably relapse after hormone–ablation therapy alone. Shionogi tumor also began to regrow around 2 weeks after castration. This regrowth was accompanied by a second wave of angiogenesis. We wondered whether VEGF was also involved in this phase of angiogenesis. By using a tetracycline-off system, Yoshiji *et al.* (20) have shown recently that beyond certain tumor size vessel growth becomes independent of VEGF and other growth factors such as basic fibroblast growth factor may stimulate angiogenesis. Thus, we were expecting basic fibroblast growth factor or another molecule involved in the regrowth of Shionogi vessels (20). Surprisingly, we found an upregulated VEGF mRNA again in the relapsed tumors (Fig. 3*B*), and no detectable basic fibroblast growth factor in either the initial or relapse phase of growth (data not shown). We cannot, however, exclude the involvement of other androgen-dependent angiogenic factors, e.g., FGF8 in the observed response (21). We speculate that hypoxia or other unidentified inducers are responsible for the second wave of VEGF production by Shionogi cells (9, 22), whereas androgen is primarily responsible for the first wave of VEGF production. The central role of VEGF in both phases of tumor growth suggests that patients with hormone-dependent tumors, in addition to hormone-independent tumors, might benefit from anti-VEGF therapy (23).

Implications. Collectively, these results suggest that castration mimics several features of anti-VEGF therapy. Following surgical or medical androgen–ablation therapy, there is a significant reduction in VEGF expression and angiogenesis in human prostate carcinomas and mammary carcinomas (1, 2, 24, 25). These tumors also become refractory to hormone–ablation therapy, similar to the Shionogi tumor. Thus, our results are significant for the treatment of human prostate and breast cancer and support the combination of anti-VEGF therapy with hormone therapy.

We thank Martin E. Gleave of the University of British Columbia for providing the Shionogi tumors, and A. Zeitman and J. Baish for their help in the early phase of this project. We also acknowledge the assistance of Sylvie Roberge and Julia Kahn in tumor and dorsal window preparations and Nils Hansen for Fig. 1. This work was supported by National Cancer Institute–Outstanding Investigator Grant R35-CA56591 to R.K.J. A.S. is a recipient of a Feodor-Lynen Fellowship from the Alexander von Humboldt Foundation (1996–1998).

1. Moon, W.-C., Choi, I. R. & Moon, S. Y. (1997) *J. Urol.*, Suppl., **157,** 223.
2. Joseph, I. B. J. K., Nelson, J. D., Denmeade, I. S. R. & Isaacs, J. T. (1997) *Clin. Cancer Res.* **3,** 2507–2512.
3. Akakura, K., Bruchovsky, N., Goldenberg, S. L., Rennie, P. S., Buckley, A. R. & Sullivan, L. D. (1993) *Cancer* **71,** 2782–2790.
4. Masai, M., Suzuki, H., Kuramochi, H., Mikami, H. & Shimazaki, J. (1994) *Endocr. J.* **41,** 709–715.
5. Halme, M., Sjoholm, B., Savola, J. M. & Scheinin, M. (1995) *Biochim. Biophys. Acta* **1266,** 207–214.
6. Leunig, M., Yuan, F., Menger, M. D., Boucher, Y., Goetz, A. E., Messmer, K. & Jain, R. K. (1992) *Cancer Res.* **52,** 6553–6560.
7. Yuan, F., Chen, Y., Dellian, M., Safabakhsh, N., Ferrara, N. & Jain, R. K. (1996) *Proc. Natl. Acad. Sci. USA* **93,** 14765–14770.
8. Melder, R. J., Koenig, G., Witwer, B. P., Safabakhsh, N., Munn, L. L. & Jain, R. K. (1996) *Nat. Med.* **2,** 992–997.
9. Alon, T., Hemo, I., Itin, A., Pe'er, J., Stone, J. & Keshet, E. (1995) *Nat. Med.* **1,** 1024–1028.
10. Shweiki, D., Itin, A., Soffer, D. & Keshet, E. (1992) *Nature (London)* **359,** 843–845.
11. Augustin, H. G., Braun, K., Telemenakis, I., Modlich U. & Kuhn, W. (1995) *Am. J. Pathol.* **147,** 339–351.
12. Modlich, U., Kaup, F. J. & Augustin, H. G. (1996) *Lab. Invest.* **74,** 771–780.
13. Benjamin, L. E. & Keshet, E. (1997) *Proc. Natl. Acad. Sci. USA* **94,** 8761–8766.
14. Carmeliet, P., Ferreira, V., Breier, G., Pollefeyt, S., Kieckens, L., Gertsenstein, M., Fahrig, M., Vandenhoeck, A., Kendraprasad, H., Eberhardt, C., *et al.* (1996) *Nature (London)* **380,** 435–439.
15. Ferrara, N., Carver-Moore, K., Chen, H., Dowd, M., Lu, L., O'Shea, K. S., Powell-Braxton, L., Hillan, K. J. & Moore, M. W. (1996) *Nature (London)* **380,** 439–442.
16. Gazit, Y., Baish, J. W., Safabakhsh, N., Leunig, M., Baxter, L. T. & Jain, R. K. (1997) *Microcirculation* **4,** 395–403.
17. Brown, L. F., Detmar, M., Claffey, K., Nagy, J. A., Feng, D. & Dvorak, A. M. (1997) in *Regulation of Angiogenesis*, eds. Goldberg, I. D. & Rosen, E. M. (Birkhäuser, Basel), pp. 233–269.
18. Hobbs, S., Monsky, W., Yuan, F., Roberts, G., Griffith, L., Torchilin, V. P. & Jain, R. K. (1998) *Proc. Natl. Acad. Sci. USA* **95,** 4607–4612.
19. Detmar, M., Brown, L. F., Schön, M. P., Elicker, B. M., Richard, L., Velasco, P., Fukumura, D., Monsky, W., Claffey, K. P. & Jain, R. K. (1998) *J. Invest. Dermatol.* **111,** 1–6.
20. Yoshiji, H., Harris, S. R. & Thorgeirsson, U. P. (1997) *Cancer Res.* **57,** 3924–3928.
21. Gosh, A. K., Shanker, D. B., Shackleford, G. M., Wu, K., T'Ang, A., Miller, G. J., Zhang, J. & Roy-Burman, P. (1996) *Cell Growth Differ.* **7,** 1425–1434.
22. Plate, K. H., Breier, G., Weich, H. A. & Risau, W. (1992) *Nature (London)* **359,** 845–848.
23. Ferrara, N. & Davis-Smyth, T. (1997) *Endocr. Rev.* **18,** 4–25.
24. Haran, E. F., Maretzek, A. F., Goldberg, I., Horowitz, A. & Degani, H. (1994) *Cancer Res.* **54,** 5511–5514.
25. Gagliardi, A. & Collins, D. C. (1993) *Cancer Res.* **53,** 533–535.